Journal of the Serbian Chemical Society
JSCS@tmf.bg.ac.rs • www.shd.org.rs/JSCS
J. Serb. Chem. Soc. 90 (4) S121–S130 (2024)
Supplementary material

SUPPLEMENTARY MATERIAL TO

Different electrode modification protocols for evaluating the water-splitting properties of a P(V)-metalloporphyrin

BOGDAN-OVIDIU TARANU*

National Institute of Research and Development for Electrochemistry and Condensed Matter, Dr. A. Paunescu Podeanu Street, No. 144, 300569 Timisoara, Romania.

J. Serb. Chem. Soc. 90 (4) (2025) 447–459

EQUATIONS

$$E_{RHE} = E_{Ag/AgCl(sat.\ KCl)} + 0.059\ pH + E°_{Ag/AgCl(sat.\ KCl)} \tag{S-1}$$

$$\eta_{OER} = E_{RHE} - 1.23 \tag{S-2}$$

$$\eta_{HER} = |E_{RHE}| \tag{S-3}$$

$$\eta = b \times \log(j) + a \tag{S-4}$$

$$j_{dl} = \frac{j_a + j_c}{2} \tag{S-5}$$

$$EASA = \frac{C_{dl} \times S_{geom}}{C_s} \tag{S-6}$$

where E_{RHE} / V is the converted potential *vs.* RHE; $E_{Ag/AgCl(sat.\ KCl)}$ / V is the measured potential *vs.* the Ag/AgCl(sat. KCl) reference electrode; $E°_{Ag/AgCl(sat.\ KCl)}$ = 0.197 V; η_{OER} / V is the O_2 evolution overpotential; η_{HER} / V is the H_2 evolution overpotential; η / V is the overpotential; j / A cm^{-2} is the current density; b / V dec^{-1} is the Tafel slope; j_{dl} / A cm^{-2} is the capacitive current density; j_a / A cm^{-2} is the absolute value of the anodic j corresponding to a given scan rate value, at an electrochemical potential value where there are only double-layer adsorption and desorption features; j_c / A cm^{-2} is the absolute value of the cathodic j corresponding to a given scan rate value, at an electrochemical potential value where there are only double-layer adsorption and desorption features; $EASA$ / cm^2 is the electrochemically active surface area; C_{dl} / F cm^{-2} is the electric double-layer capacitance; S_{geom} / cm^2 is the geometric surface of the electrode and C_s / F cm^{-2} is the specific capacitance.[1-4]

* Corresponding author. E-mail: b.taranu84@gmail.com

ELECTROCHEMISTRY DATA

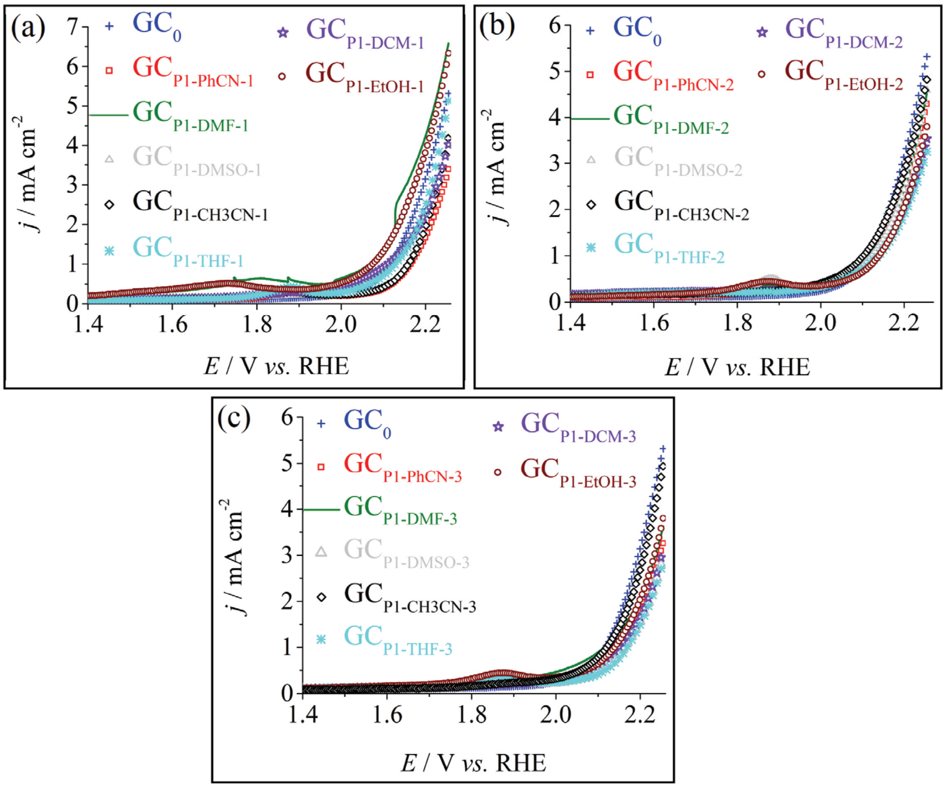

Fig. S-1. Anodic polarization curves recorded on GC$_0$ and on (a) GC$_{P1-PhCN-1}$, GC$_{P1-DMF-1}$, GC$_{P1-DMSO-1}$, GC$_{P1-CH3CN-1}$, GC$_{P1-THF-1}$, GC$_{P1-DCM-1}$ and GC$_{P1-EtOH-1}$; (b) GC$_{P1-PhCN-2}$, GC$_{P1-DMF-2}$, GC$_{P1-DMSO-2}$, GC$_{P1-CH3CN-2}$, GC$_{P1-THF-2}$, GC$_{P1-DCM-2}$ and GC$_{P1-EtOH-2}$ and (c) on GC$_{P1-PhCN-3}$, GC$_{P1-DMF-3}$, GC$_{P1-DMSO-3}$, GC$_{P1-CH3CN-3}$, GC$_{P1-THF-3}$, GC$_{P1-DCM-3}$ and GC$_{P1-EtOH-3}$. Electrolyte solution: 0.1 mol L^{-1} H_2SO_4. v = 5 mV s^{-1}.

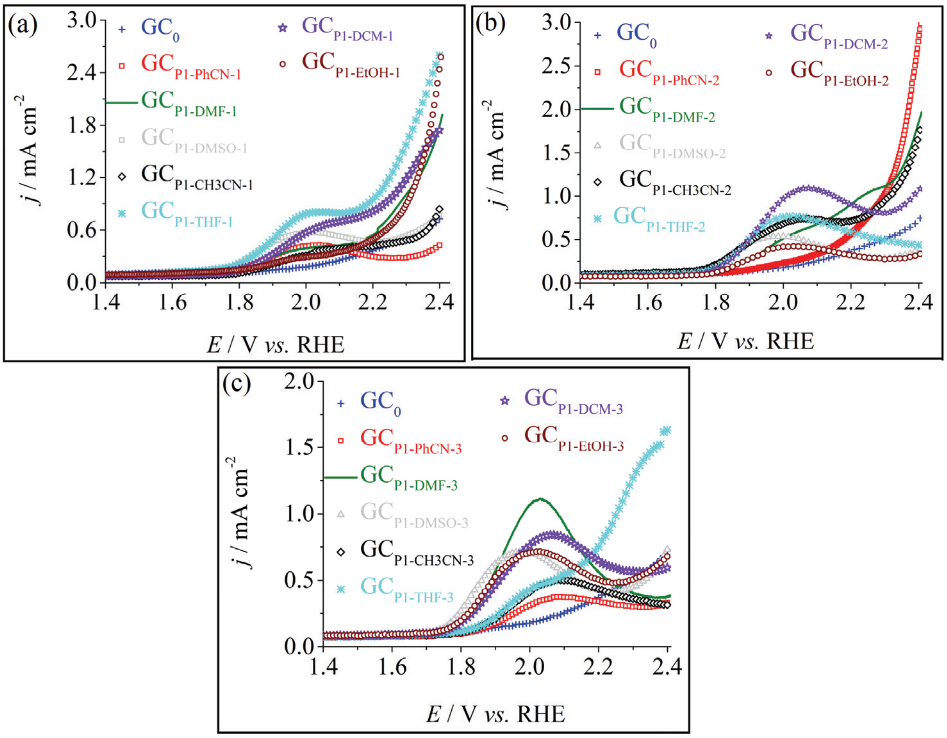

Fig. S-2. Anodic polarization curves recorded on GC_0 and on (a) $GC_{P1-PhCN-1}$, $GC_{P1-DMF-1}$, $GC_{P1-DMSO-1}$, $GC_{P1-CH3CN-1}$, $GC_{P1-THF-1}$, $GC_{P1-DCM-1}$ and $GC_{P1-EtOH-1}$; (b) $GC_{P1-PhCN-2}$, $GC_{P1-DMF-2}$, $GC_{P1-DMSO-2}$, $GC_{P1-CH3CN-2}$, $GC_{P1-THF-2}$, $GC_{P1-DCM-2}$ and $GC_{P1-EtOH-2}$ and (c) on $GC_{P1-PhCN-3}$, $GC_{P1-DMF-3}$, $GC_{P1-DMSO-3}$, $GC_{P1-CH3CN-3}$, $GC_{P1-THF-3}$, $GC_{P1-DCM-3}$ and $GC_{P1-EtOH-3}$. Electrolyte solution: 0.1 mol L^{-1} KCl. $v = 5$ mV s^{-1}.

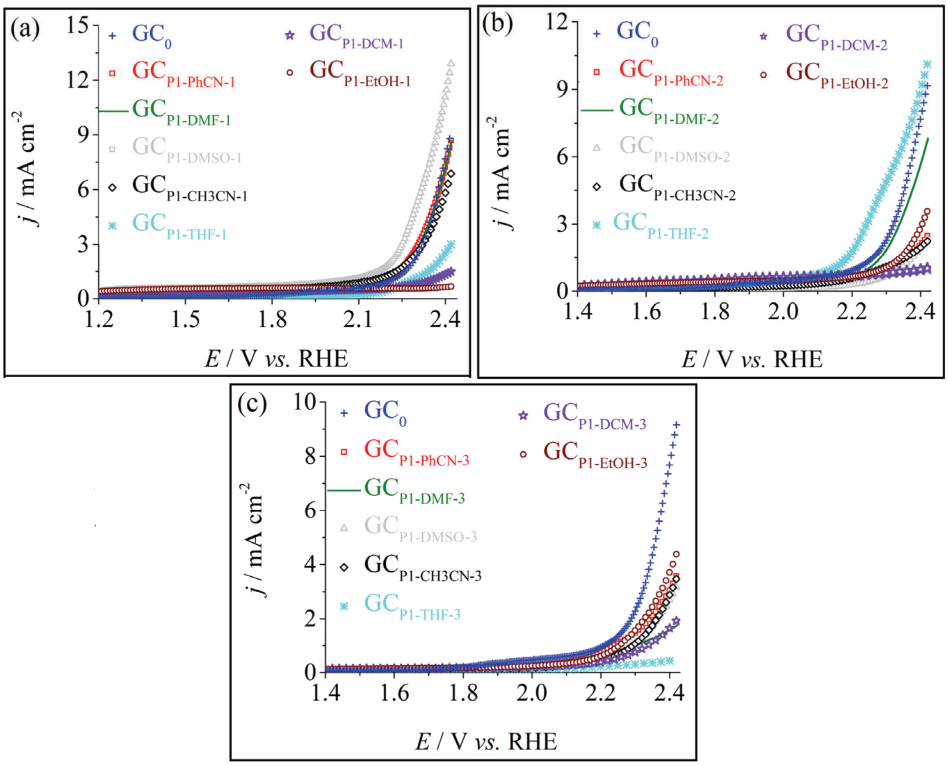

Fig. S-3. Anodic polarization curves recorded on GC_0 and on (a) $GC_{P1\text{-}PhCN\text{-}1}$, $GC_{P1\text{-}DMF\text{-}1}$, $GC_{P1\text{-}DMSO\text{-}1}$, $GC_{P1\text{-}CH3CN\text{-}1}$, $GC_{P1\text{-}THF\text{-}1}$, $GC_{P1\text{-}DCM\text{-}1}$ and $GC_{P1\text{-}EtOH\text{-}1}$; (b) $GC_{P1\text{-}PhCN\text{-}2}$, $GC_{P1\text{-}DMF\text{-}2}$, $GC_{P1\text{-}DMSO\text{-}2}$, $GC_{P1\text{-}CH3CN\text{-}2}$, $GC_{P1\text{-}THF\text{-}2}$, $GC_{P1\text{-}DCM\text{-}2}$ and $GC_{P1\text{-}EtOH\text{-}2}$ and (c) on $GC_{P1\text{-}PhCN\text{-}3}$, $GC_{P1\text{-}DMF\text{-}3}$, $GC_{P1\text{-}DMSO\text{-}3}$, $GC_{P1\text{-}CH3CN\text{-}3}$, $GC_{P1\text{-}THF\text{-}3}$, $GC_{P1\text{-}DCM\text{-}3}$ and $GC_{P1\text{-}EtOH\text{-}3}$. Electrolyte solution: 1 mol L^{-1} KOH. v = 5 mV s^{-1}.

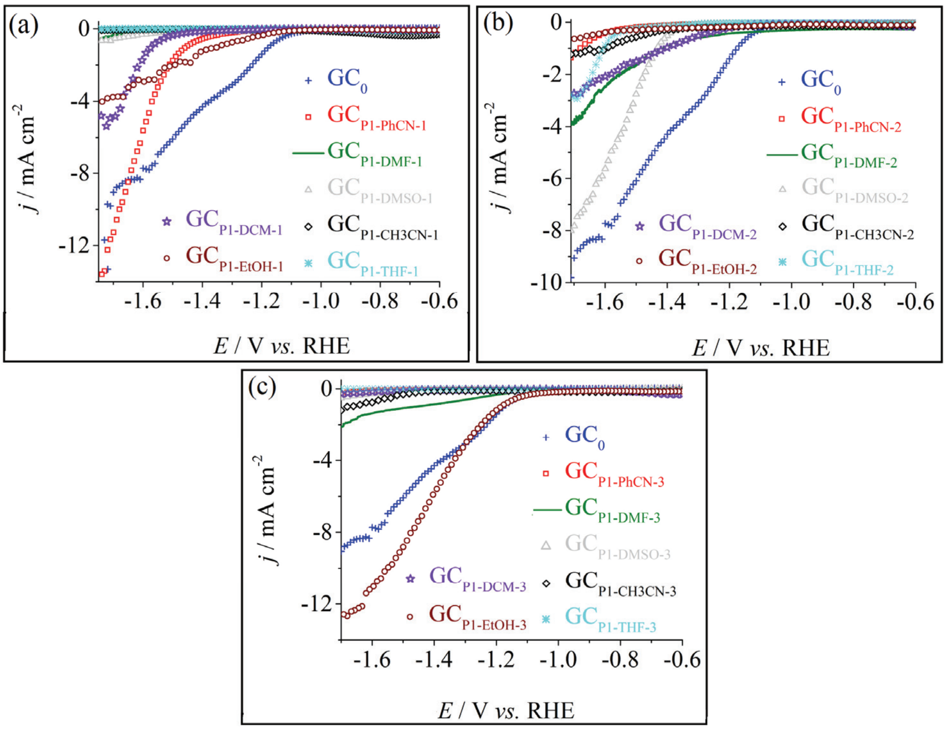

Fig. S-4. Cathodic polarization curves recorded on GC$_0$ and on (a) GC$_{P1-PhCN-1}$, GC$_{P1-DMF-1}$, GC$_{P1-DMSO-1}$, GC$_{P1-CH3CN-1}$, GC$_{P1-THF-1}$, GC$_{P1-DCM-1}$ and GC$_{P1-EtOH-1}$; (b) GC$_{P1-PhCN-2}$, GC$_{P1-DMF-2}$, GC$_{P1-DMSO-2}$, GC$_{P1-CH3CN-2}$, GC$_{P1-THF-2}$, GC$_{P1-DCM-2}$ and GC$_{P1-EtOH-2}$ and (c) on GC$_{P1-PhCN-3}$, GC$_{P1-DMF-3}$, GC$_{P1-DMSO-3}$, GC$_{P1-CH3CN-3}$, GC$_{P1-THF-3}$, GC$_{P1-DCM-3}$ and GC$_{P1-EtOH-3}$. Electrolyte solution: 0.1 mol L^{-1} H_2SO_4. v = 5 mV s^{-1}.

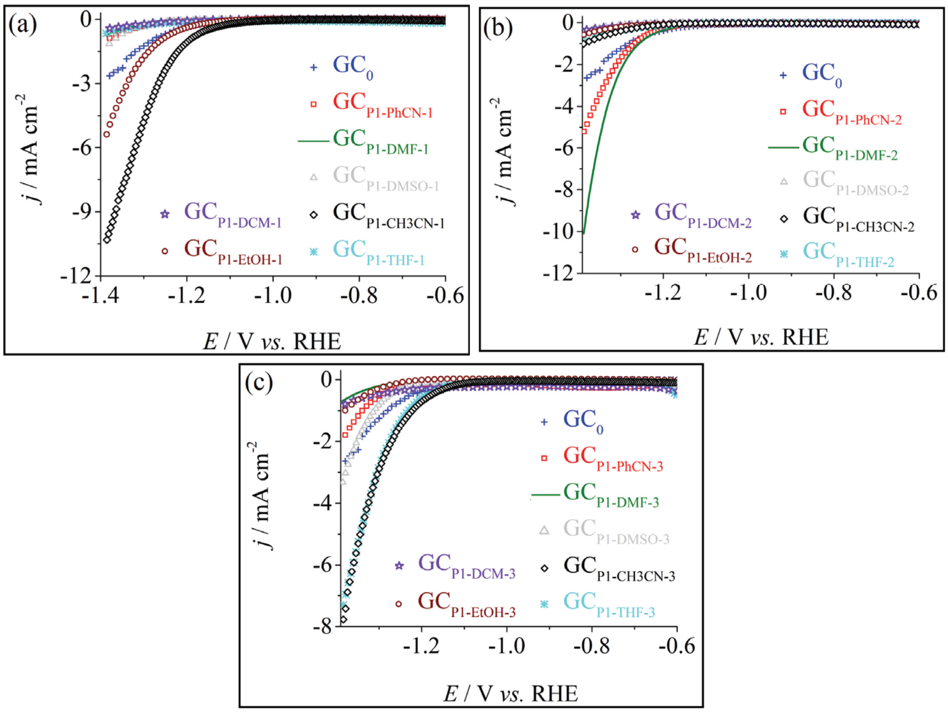

Fig. S-5. Cathodic polarization curves recorded on GC$_0$ and on (a) GC$_{P1-PhCN-1}$, GC$_{P1-DMF-1}$, GC$_{P1-DMSO-1}$, GC$_{P1-CH3CN-1}$, GC$_{P1-THF-1}$, GC$_{P1-DCM-1}$ and GC$_{P1-EtOH-1}$; (b) GC$_{P1-PhCN-2}$, GC$_{P1-DMF-2}$, GC$_{P1-DMSO-2}$, GC$_{P1-CH3CN-2}$, GC$_{P1-THF-2}$, GC$_{P1-DCM-2}$ and GC$_{P1-EtOH-2}$ and (c) on GC$_{P1-PhCN-3}$, GC$_{P1-DMF-3}$, GC$_{P1-DMSO-3}$, GC$_{P1-CH3CN-3}$, GC$_{P1-THF-3}$, GC$_{P1-DCM-3}$ and GC$_{P1-EtOH-3}$. Electrolyte solution: 0.1 mol L^{-1} KCl. v = 5 mV s^{-1}.

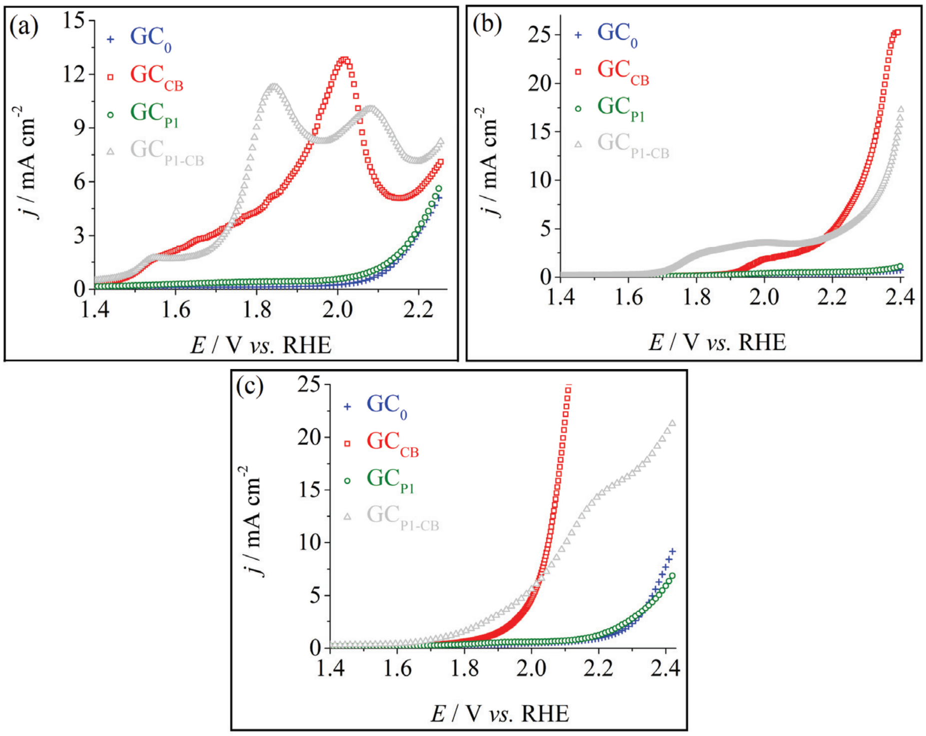

Fig. S-6. Anodic polarization curves recorded on GC_0, GC_{CB}, GC_{P1} and GC_{P1-CB} in the following electrolyte solutions: (a) 0.1 mol L^{-1} H_2SO_4, (b) 0.1 mol L^{-1} KCl and (c) 1 mol L^{-1} KOH. v = 5 mV s^{-1}.

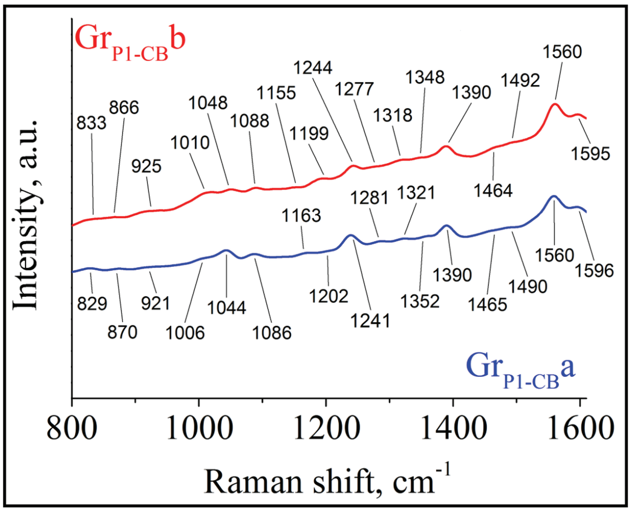

Fig. S-7. Raman spectra recorded on GC_{P1-CB} before a cathodic stability experiment performed in 1 mol L^{-1} KOH solution (GC_{P1-CB}a) and after the experiment (GC_{P1-CB}b).

TABLES

TABLE S-I. The HER activity of $GC_{P1\text{-}CB}$ and of other porphyrin-based electrodes

Catalyst @substrate	Environment	η_{HER} / mV at j = -10 mA cm^{-2}	Tafel slope, mV dec^{-1}	Ref.
Zn-TPP/G @Cu foil [a]	0.5 mol L^{-1} H_2SO_4	~ 480 [b]	-	5
Zn-TAPP/G @Cu foil [c]	0.5 mol L^{-1} H_2SO_4	~ 480 [b]	-	5
Zn-TPyP/G @Cu foil [d]	0.5 mol L^{-1} H_2SO_4	~ 560 [b]	-	5
ZnTAPP-NA @GC [e]	1 mol L^{-1} KOH	546	121	6
CoTAPP-NA @GC [f]	1 mol L^{-1} KOH	470	110	6
CoTPP-SD @CFP [g]	1 mol L^{-1} KOH	475	-	7
CoCOP @CFP [h]	1 mol L^{-1} KOH	310	161	7
CoTCPP @FTO/Ag [i]	0.5 mol L^{-1} H_2SO_4	666	264	8
CoTCPP polymer @FTO/Ag [j]	0.5 mol L^{-1} H_2SO_4	475	197	8
CoTMPyP/ERGO @GC [k]	0.1 mol L^{-1} KOH	347 [l]	99	9
CoTMPyP/ERGO @GC	1 mol L^{-1} KOH	315 [l]	96	9
Co-2DP @Ti foil [m]	1 mol L^{-1} KOH	367 [l]	126	10
CoP-2ph-CMP-800 @GC [n]	1 mol L^{-1} KOH	360	121	11
CoP-3ph-CMP-800 @GC [o]	1 mol L^{-1} KOH	380	-	11
CoP-4ph-CMP-800 @GC [p]	1 mol L^{-1} KOH	440	-	11
$G_{ZnP\text{-}DMF\text{-}1}$ [q]	1 mol L^{-1} KOH	520	150	2
Porphvlar-based ink @carbon paper [r]	1 mol L^{-1} PBS	~ 770 [s]	227	12
$G_{CB\text{-}PZn}$ [t]	0.1 mol L^{-1} KCl	1020	249	3
Fe-porphyrin polymer @carbon paper [u]	1 mol L^{-1} KOH	678	363	13
Co-porphyrin polymer @carbon paper [v]	1 mol L^{-1} KOH	437	195	13
Ni-porphyrin polymer @carbon paper [w]	1 mol L^{-1} KOH	644	345	13

Cu-porphyrin polymer @carbon paper [x]	1 mol L^{-1} KOH	436	236	[13]
Pt-TAPP/G @Cu foil [y]	0.5 mol L^{-1} H_2SO_4	~ 550	-	[5]
2H-TAPP/G @Cu foil [z]	0.5 mol L^{-1} H_2SO_4	600 [aa]	-	[5]
Ni-TAPP/G @Cu foil [ab]	0.5 mol L^{-1} H_2SO_4	600 [s]	-	[5]
$G_{P2\text{-}DMF}$ [ac]	0.5 mol L^{-1} H_2SO_4	108	205	[14]
$G_{P4\text{-}NiPh\text{-}THF}$ [ad]	1 mol L^{-1} KOH	430	140	[15]
$[ERGO/CoTMPyP]_7$/ PDDA/4-ABA@GC [ae]	0.1 mol L^{-1} KOH	474 [l]	116	[16]
$GC_{P1\text{-}CB}$	1 mol L^{-1} KOH	770	135	This work

[a] Zn-TPP = 5,10,15,20-tetraphenyl-21H,23H-porphine on single-layer graphene; [b] at -3 mA cm^{-2}; [c] Zn-TAPP = 5,10,15,20-tetrakis(4-aminophenyl)-21H,23H-porphine on single-layer graphene; [d] Zn-TPyP = 5,10,15,20-tetrakis(4-pyridyl)-21H,23H-porphine on single-layer graphene; [e] ZnTAPP-NA = Zn(II) 5,10,15,20-tetra(4-aminophenyl)-21H,23H-porphyrin - ferrocene-1,1'-dicarbaldehyde; [f] CoTAPP-NA = Co(II) 5,10,15,20-tetra(4-aminophenyl)-21H,23H-porphyrin - ferrocene-1,1'-dicarbaldehyde; [g] CoTPP-SD@CFP = Co(II) 5,10,15,20-tetrakis(4-aminophenyl)porphyrin – salicylaldehyde@carbon fibre paper; [h] CoCOP = Co(II) 5,10,15,20-tetrakis(4-aminophenyl)porphyrin-based covalent organic polymer; [i] CoTCPP = Co(II) meso-tetra(4-carboxyphenyl)porphyrin; [j] CoTCPP polymer = crystalline Co(II) meso-tetra(4-carboxyphenyl)porphyrin-based polymeric system; [k] CoTMPyP/ERGO = tetrakis(N-methylpyridyl)porphyrinato cobalt / electrochemically reduced graphene oxide; [l] at -1 mA cm^{-2}; [m] Co-2DP = multilayer 2D polymer based on Co(II) 5,10,15,20-tetrakis(4-aminophenyl)-21H,23H-porphyrin and 2,5-dihydroxyterephthalaldehyde; [n] CoP-2ph-CMP-800, [o] CoP-3ph-CMP-800 and [p] CoP-4ph-CMP-800 = conjugated mesoporous polymer based on Co-porphyrins and pyrolyzed at 800 °C; $[ERGO/CoTMPyP]_7$/PDDA/4-ABA@GC = multilayer films containing tetrakis(N-methylpyridyl)porphyrinato cobalt, on treated glassy carbon electrode; [q] $G_{ZnP\text{-}DMF\text{-}1}$ = Zn(II) 5,10,15,20-tetrakis(4-pyridyl)-porphyrin drop-casted from DMF in one layer on graphite; [r] Porphvlar = organic polymer obtained from the condensation of terephthaloyl chloride and 5,10,15,20-tetrakis(4-aminophenyl)porphyrin; [s] at -7 mA cm^{-2}; [t] $G_{CB\text{-}PZn}$ = Zn(II) 5-(4-pyridyl)-10,15,20-tris(4-phenoxyphenyl)-porphyrin and Carbon Black drop-casted as catalyst ink on graphite; [u,v,w,x] Fe-porphyrin polymer, Co-porphyrin polymer, Ni-porphyrin polymer, Cu-porphyrin polymer = organic polymers obtained from the polymerization reaction of poly(*p*-phenylene terephtalamide) with 5,10,15,20-tetrakis(4-aminophenyl)porphyrin metalated with Fe, Co, Ni and Cu; [y] Pt-TAPP/G = Pt(II) 5,10,15,20-tetrakis-(4-aminophenyl)-21H,23H-porphine on single-layer graphene; [z] 2H-TAPP/G = 5,10,15,20-tetrakis-(4-aminophenyl)-21H,23H-porphine on single-layer graphene; [aa] at -9 mA cm^{-2}; [ab] Ni-TAPP/G = Ni(II) 5,10,15,20-tetrakis-(4-aminophenyl)-21H,23H-porphine on single-layer graphene; [ac] $G_{P2\text{-}DMF}$ = Pt(II) 5-(3-hydroxyphenyl)-10,15,20-tris(3-methoxyphenyl)-porphyrin drop-casted on graphite substrate from N,N-dimethylformamide; [ad] $G_{P4\text{-}NiPh\text{-}THF}$ = graphite substrate modified with suspension of nickel phosphite in solution of 5,10,15,20-tetrakis(4-methoxyphenyl)porphyrin dissolved in tetrahydrofuran; [ae] $[ERGO@CoTMPyP]_7$/PDDA/4-ABA@GC = multilayer films containing tetrakis(N-methylpyridyl)porphyrinato cobalt, on treated glassy carbon electrode.

REFERENCES

1. B.-O. Taranu, E. Fagadar-Cosma, *Processes* **10** (2022) 1 (https://doi.org/10.3390/pr10030611)
2. B.-O. Taranu, E. Fagadar-Cosma, *Nanomaterials-Basel* **12** (2022) 1 (https://doi.org/10.3390/nano12213788)
3. B.-O. Taranu, S. F. Rus, E. Fagadar-Cosma, *Coatings* **14** (2024) 1 (https://doi.org/10.3390/coatings14081048)
4. B. O. Taranu, S. D. Novaconi, M. Ivanovici, J. N. Goncalves, F. S. Rus, *Appl. Sci.-Basel* **12** (2022) 1 (https://doi.org/10.3390/app12136821)
5. S. Seo, K. Lee, M. Min, Y. Cho, M. Kim, H. Lee, *Nanoscale* **9** (2017) 3969 (https://doi.org/10.1039/C6NR09428G)
6. G. Cai, L. Zeng, L. He, S. Sun, Y. Tong, J. Zhang, *Chem.-Asian J.* **15** (2020) 1963 (https://doi.org/10.1002/asia.202000083)
7. A. Wang, L. Cheng, W. Zhao, X. Shen, W. Zhu, *J. Colloid Interf. Sci.* **579** (2020) 598 (10.1016/j.jcis.2020.06.109)
8. Y. Wu, J. M. Veleta, D. Tang, A. D. Price, C. E. Botez, D. Villagran, *Dalton T.* **47** (2018) 8801 (https://doi.org/10.1039/C8DT00302E)
9. J. Ma, L. Liu, Q. Chen, M. Yang, D. Wang, Z. Tong, Z. Chen, *Appl. Surf. Sci.* **399** (2017) 535 (https://doi.org/10.1016/j.apsusc.2016.12.070)
10. H. Sahabudeen, H. Qi, B. A. Glatz, D. Tranca, R. Dong, Y. Hou, T. Zhang, C. Kuttner, T. Lehnert, G. Seifert, U. Kaiser, A. Fery, Z. Zheng, X. Feng, *Nat. Commun.* **7** (2016) 1 (https://doi.org/10.1038/ncomms13461)
11. H. Jia, Y. Yao, Y. Gao, D. Lu, P. Du, *Chem. Commun.* **52** (2016) 13483 (https://doi.org/10.1039/C6CC06972J)
12. Y. Ge, Z. Lyu, M. Marcos-Hernandez, D. Villagran, *Chem. Sci.* **13** (2022) 8597 (https://doi.org/10.1039/D2SC01250B)
13. N. Ocuane, Y. Ge, C. Sandoval-Pauker, D. Villagran, *Dalton T.* **53** (2024) 2306 (https://doi.org/10.1039/D3DT03371F)
14. I. Fratilescu, A. Lascu, B. O. Taranu, C. Epuran, M. Birdeanu, A.-M. Macsim, E. Tanasa, E. Vasile, E. Fagadar-Cosma, *Nanomaterials-Basel* **12** (2022) 1 (https://doi.org/10.3390/nano12111930)
15. B.-O. Taranu, E. Fagadar-Cosma, P. Sfirloaga, M. Poienar, *Energies* **16** (2023) 1 (https://doi.org/10.3390/en16031212)
16. D. Huang, J. Lu, S. Li, Y. Luo, C. Zhao, B. Hu, M. Wang, Y. Shen, *Langmuir* **30** (2014) 6990 (https://doi.org/10.1021/la501052m).